analytical chemistry

ARTICLE

pubs.acs.org/ac

# Designing Electrochemical Interfaces with Functionalized Magnetic Nanoparticles and Wrapped Carbon Nanotubes as Platforms for the Construction of High-Performance Bienzyme Biosensors

Marcos Eguílaz, Reynaldo Villalonga, Paloma Yáñez-Sedeño, and José M. Pingarrón*

Department of Analytical Chemistry, Faculty of Chemistry, University Complutense of Madrid, 28040 Madrid, Spain

Supporting Information

**ABSTRACT:** The design of a novel biosensing electrode surface, combining the advantages of magnetic ferrite nanoparticles (MNPs) functionalized with glutaraldehyde (GA) and poly(diallyldimethylammonium chloride) (PDDA)-coated multiwalled carbon nanotubes (MWCNTs) as platforms for the construction of high-performance multienzyme biosensors, is reported in this work. Before the immobilization of enzymes, GA-MNP/PDDA/MWCNT composites were prepared by wrapping of carboxylated MWCNTs with positively charged PDDA and interaction with GA-functionalized MNPs. The nanoconjugates were characterized by scanning electron microscopy (SEM) and electrochemistry. The electrode platform was used to construct a bienzyme biosensor for the determination of cholesterol, which implied coimmobilization of cholesterol oxidase (ChOx) and peroxidase (HRP) and the use of hydroquinone as redox mediator. Optimization of all variables involved in the preparation and analytical performance of the bienzyme electrode was accomplished. At an applied potential of −0.05 V, a linear calibration graph for cholesterol was obtained in the 0.01−0.95 mM concentration range. The detection limit (0.85 $\mu$M), the apparent Michaelis−Menten constant (1.57 mM), the stability of the biosensor, and the calculated activation energy can be advantageously compared with the analytical characteristics of other CNT-based cholesterol biosensors reported in the literature. Analysis of human serum spiked with cholesterol at different concentration levels yielded recoveries between 100% and 103%

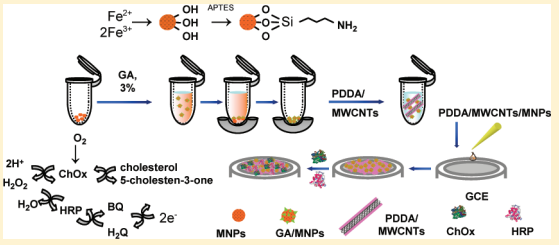


The search for electrode interfaces able to conjugate an efficient immobilization of biomolecules with a high electroanalytical performance in terms of sensitivity, rapidity of transducer response, and easy real applicability is a challenge in the field of advanced electrochemical biosensors. The use of nanostructured electrode surfaces with carbon nanotubes (CNTs) or metal nanoparticles for such a purpose is well documented in the recent literature.[1] However, electrode modification with magnetic nanoparticles (MNPs) for implementing efficient bioelectrodes is a much less explored area, although MNPs constitute a very interesting material for the construction of biosensing devices because of their high biocompatibility and protein load capacity[2] The large surface area provided by MNPs for biomolecules attachment makes them extremely useful for purification and/or preconcentration purposes, which usually leads to enhanced detection sensitivity. Moreover, their magnetism makes the biosensors construction steps much easier by application of an external magnetic field (see below). Other advantages, in comparison with metal nanoparticles, are nontoxicity and ease of preparation. In particular, various applications to the preparation of electrochemical enzyme biosensors have been reported in the last years. For example, a sensitive tyrosinase biosensor based on magnetic $Fe_3O_4$-coated CNTs was prepared and applied to the detection of coliforms by use of a flow injection system. In this design, the electrode surface for enzyme immobilization was fabricated by dispersing polystyrene sulfonate (PSS) -wrapped multiwalled CNTs (MWCNTs) in poly(diallydimethylammonium chloride) (PDDA) and further incorporation of $Fe_3O_4$ magnetic nanoparticles by mixing with PDDA/MWCNT solution and ultrasonication for 1 h.[3] Another reported configuration involved chemical coprecipitation of $Fe^{2+}$ and $Fe^{3+}$ in alkaline solution in the presence of CNTs and chitosan (Chit) to give CNTs/$Fe_3O_4$/Chit. Then, the composite was dispersed in glucose oxidase (GOx) solution and cross-linked with glutaraldehyde to prepare a glucose biosensor. The intense electrocatalytic activity toward hydrogen peroxide allowed the low-potential amperometric biosensing of glucose.[4] Another glucose biosensor was also described that made use of MWCNTs decorated with silicon dioxide-coated magnetic nanoparticles on a glassy carbon electrode. The GOx biosensor was prepared by deposition of the enzyme over Nafion-solubilized $Fe_3O_4$/$SiO_2$/MWCNT electrode.[5] Also, a novel glucose biosensor was prepared with $Fe_3O_4$ nanoparticles, Prussian Blue, and GOx attracted to the surface of solid paraffin carbon paste electrode by magnetic force. GOx was covalently conjugated to the amine-modified nanoparticles.[6] Magnetic $Fe_3O_4$

**Received:** June 9, 2011
**Accepted:** September 10, 2011
**Published:** September 11, 2011

  

nanoparticles were used to prepare a disposable glucose biosensor by drop-coating of ferricyanide−$Fe_3O_4$ mixture onto the surface of screen-printed carbon electrodes (SPCEs) and layering on GOx.[7] Another example is that based on simple mixing of GOx with $Fe_3O_4$ nanoparticles, cross-linking on a Pt electrode with Chit medium by glutaraldehyde, and coating with a thin Nafion film.[8]

Not only enzyme electrodes have been prepared with magnetic nanoparticles and CNTs. For instance, a highly sensitive electrochemical immunosensor was developed by immobilization of both tyrosinase and magnetic nanoparticles onto the surface of CNTs by covalent attachment, followed by additional cross-linking via glutaraldehyde to construct multilayered tyrosinase−magnetic nanopartícles aggregates. Then, a primary antibody against a target analyte of hIgG was immobilized and used for a sandwich-type immunoassay with a secondary antibody conjugated with alkaline phosphatase.[9]

On the other hand, PDDA is a water-soluble, quaternary ammonium cationic polyelectrolyte with adhesion and film-forming properties; it is a positively charged colloid when dissolved in aqueous solutions.[10−12] It has been used as a dispersant of CNTs since positively charged PDDA can easily coat the negatively charged surface of carboxylated CNTs, conferring water solubility and solution stability to PDDA-coated CNTs through electrostatic mechanism. The layer-by-layer (LBL) assembling approach using CNTs and PDDA has been used to prepare various enzyme biosensor configurations.[13,14] The adhesion and film-forming properties of PDDA play an essential role in the construction of stable and useful biointerfaces.

The aim of this work is to design a novel biosensing electrode surface, combining the advantages of functionalized MNPs and PDDA-coated CNTs, suitable to construct multienzyme biosensors with enhanced analytical performance with respect to CNT-based designs. To our knowledge, this strategy is reported for the first time in this work. As the target analyte to evaluate the capabilities of this new electrochemical interface, we selected cholesterol due to the well-documented existing literature on cholesterol biosensors involving immobilization of the enzyme cholesterol oxidase (ChOx) on different electrode substrates.[15] Nanocomposite films of polyaniline (PANI) and multiwalled carbon nanotubes (MWCNTs) on indium tin oxide (ITO) -coated glass plates with further covalent immobilization of ChOx were used to prepare an electrochemical cholesterol biosensor.[16] Also, an ITO-coated glass electrode modified with gold nanoparticles (AuNPs) electrodeposited onto thiol functionalized MWCNTs was used to construct an amperometric biosensor in which ChOx was immobilized onto a cross-linked matrix of Chit and a room-temperature ionic liquid.[17] MWCNTs dispersed in a Pt nanoparticle-doped Chit solution were utilized to form stable ultrathin multilayer films on gold electrodes where ChOx was immobilized by use of glutaric dialdehyde.[18] Nickel hexacyanoferrate nanoparticles (NiNP) attached to MWCNTs through histidine have been also used to immobilize ChOx on a glassy carbon electrode (GCE).[19] Pt nanoparticles electrochemically deposited onto a MWCNT/Chit matrix were also employed to prepare a ChOx biosensor.[20] Furthermore, a sol−gel Chit/$SiO_2$ and MWCNT organic−inorganic hybrid composite was used for the immobilization of ChOx on the surface of a Prussian Blue-modified GCE.[21] Finally, a MWCNT/sol−gel-derived $SiO_2$/Chit nanobiocomposite, where cholesterol esterase (ChEt) and ChOx were coimmobilized with glutaraldehyde, was reported for determination of total cholesterol.[22]

Moreover, the direct electrochemistry of ChOx was observed on the surface of a multilayer ChOx/MWCNT prepared onto a PDDA-modified graphite electrode[123] An amperometric cholesterol biosensor was fabricated through LBL deposition of PDDA and ChOx on MWNTs-modified gold electrode, followed by electrochemical generation of a nonconducting poly(*o*-phenylenediamine) (PPD) film as protective coating.[24]

Therefore, according to the aim of this work, we developed a bienzyme biosensor by coimmobilization of ChOx and horseradish peroxidase (HRP) onto a MNP/PDDA/MWCNT-modified GCE. Magnetic ferrite nanoparticles were functionalized previously with glutaraldehyde to improve the immobilization of the enzymes onto the composite material. Moreover, the coimmobilization of HRP and the use of hydroquinone as a redox mediator allowed a low detection potential for $H_2O_2$ to be used, thus increasing the selectivity of the method and avoiding the accumulation of $H_2O_2$, which causes ChOx inactivation.

## EXPERIMENTAL SECTION

**Chemicals and Solutions.** Multiwalled carbon nanotubes (MWCNTs, 30 ± 15 nm ø) with 95% purity were supplied from NanoLab, Brighton, MA. Poly(diallydimethylammonium chloride) (PDDA) (20% w/w in water) was from Sigma−Aldrich. Cholesterol oxidase from *Brevibacterium* sp. (Sigma, 34 units/mg of solid) was used. Lyophilized powder (500 units) was dissolved in 1.0 mL of 0.1 M phosphate-buffered saline (PBS), pH 7.4, and from this, aliquots were prepared and frozen at −50 °C until use. Horseradish peroxidase (HRP) type II (Sigma, 188 units/mg of solid) was also employed. Solutions containing 1880 units·$mL^{-1}$ were prepared in 0.1 M PBS, pH 7.4. Stock 0.02 M solutions of cholesterol were prepared by dissolving 0.0386 g of the product (Sigma, 99%) by gentle stirring in 0.2 mL of aqueous Triton X-100 (Merck) at 60 °C and dilution with 0.1 M phosphate buffer solution of pH 7.5 up to a volume of 5.0 mL. More diluted cholesterol standard solutions were prepared from this by use of 0.1 M phosphate buffer solution of pH 7.5 containing 1% Triton X-100 (PBS). An 0.1 M PBS solution containing 1% Triton X-100 was also used as supporting electrolyte. Hydrogen peroxide (100 mM; Scharlau, 35%) and 100 mM hydroquinone (HQ) (Sigma) solutions were prepared daily by dilution in 0.1 M PBS, pH 7.5. Glutaraldehyde (GA, Aldrich, 25%) solutions were prepared by dilution in 0.1 M PBS of pH 7.5. (3-Aminopropyl)triethoxysilane (APTES) was acquired from Sigma−Aldrich. All chemicals were of analytical reagent grade, and the water used was obtained from a Milli-Q purification system (Millipore, Bedford, MA). The analyzed samples were lyophilized human serum (Sigma) spiked with cholesterol.

**Electrochemical Instrument and Electrodes.** Amperometric and voltammetric measurements were carried out with a BAS 100 B potentiostat (West Lafayette, IN) provided with a BAS C2 EF-1080 cell stand and controlled by BAS 100 W 2.0 electrochemical analysis software. A three-electrode (BAS VC-2 5-mL) glass electrochemical cell was used. The electrochemical biosensor with a Metrohm 6.084.010 glassy carbon electrode (3 mm ø) as electrode substrate was used as the working electrode. The reference electrode was an Ag/AgCl/KCl 3 M BAS MF 2063, and a BAS MW 1032 Pt wire was used as the auxiliary electrode. Electrochemical impedance measurements were performed on a $\mu$-Autolab type III with FRA2 software (Ecochemie).

**Preparation of PDDA/MWCNTs.** MWCNTs were chemically shortened and carboxylated by treatment with a 3:1 mixture of

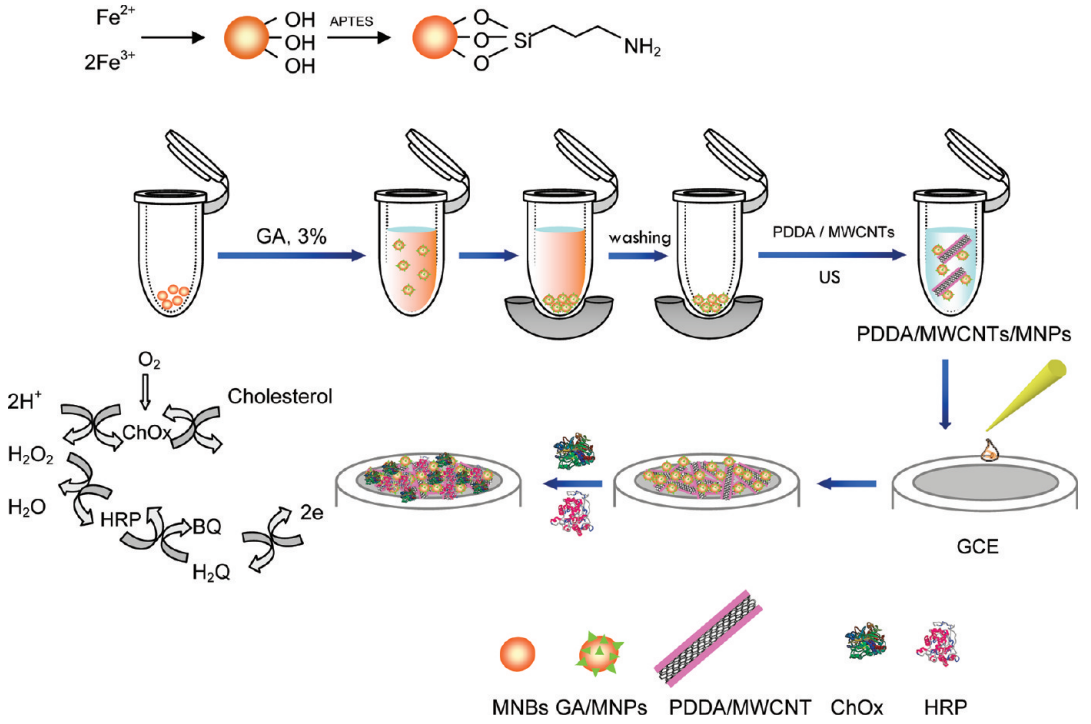


**Figure 1.** Steps involved in the construction and functioning of the HRP/ChOx/GA-MNP/PDDA/MWCNT/GCE biosensor.

sulfuric and nitric acids under ultrasonic stirring for 5 h. The resulting product was centrifuged at 14 000 rpm and exhaustively washed with distilled water. Functionalization of MWCNTs with PDDA was carried out by dispersion of 10 mg of carboxylated MWCNTs in 20 mL of a 0.25% PDDA aqueous solution containing 0.5 M NaCl and sonicated for 30 min.[25] The resulting dispersion was centrifuged at 14 000 rpm and washed three times with water. Finally, 4 mg of dry PDDA/MWCNTs were dispersed in 5 mL of water and the resulting solution was sonicated for 5 min before use.

**Preparation of Glutaraldehyde-Functionalized $Fe_3O_4$/APTES Magnetic Nanoparticles.** $Fe_3O_4$ magnetic nanoparticles were prepared by following the method described in the literature[26] with little modification. Briefly, 5.4 g of $FeCl_3 \cdot 6H_2O$ and 2.0 g of $FeCl_2 \cdot 4H_2O$ were dissolved in 25 mL of 0.5 M HCl under $N_2$ atmosphere. Then, drops of this solution were continuously added to 250 mL of a 1.5 M NaOH solution with vigorous mechanical stirring and ultrasound treatment under continuous $N_2$ bubbling. The black precipitate formed was isolated by magnetic decantation, exhaustively washed with double-distilled water until neutrality, and further washed twice with ethanol and dried under vacuum. Via this protocol, quasi-spherical magnetic nanoparticles with average size of $14 \pm 7$ nm were obtained, as revealed by transmission electron microscopy (TEM).[27] The core−shell $Fe_3O_4$/APTES nanoparticles (MNPs) were prepared as previously reported[28] by dispersing 300 mg of the synthesized $Fe_3O_4$ nanoparticles in a mixture of 600 mL of ethanol and 4 mL of water by sonication. APTES (120 $\mu$L) was then added, and the mixture was mechanically stirred under $N_2$ atmosphere for 7 h. The nanoparticles were separated by magnetic decantation and purified by five cycles of redispersion in ethanol and magnetic decantation. MNPs were finally dried at room temperature under vacuum. The core−shell $Fe_3O_4$/APTES nanoparticles showed similar shape to the uncoated material, with a slightly larger size, $17 \pm 9$ nm, due to the polysiloxane coverage.[27] Glutaraldehyde-functionalized MNPs (GA-MNPs) were prepared by dispersing 1 mg of $Fe_3O_4$/APTES nanoparticles in 1 mL of 3% glutaraldehyde solution in sodium phosphate buffer, pH 7.5. The mixture was mechanically stirred for 2 h, and the modified nanoparticles were magnetically decanted and sequentially washed four times with distilled water. The resulting solid was finally dried at room temperature.

**Preparation of HRP/ChOx/GA-MNP/PDDA/MWCNT/GCE Biosensor.** First, the GCE surface was polished with 0.3 $\mu$m alumina slurries, rinsed thoroughly with deionized water, sonicated for 30 s in water and 30 s in acetone, and dried in air. Then, GA-MNP/PDDA/MWCNT conjugate was prepared by addition of 1 mg of GA-MNPs to 500 $\mu$L of the PDDA/MWCNT dispersion and sonicated for 5 min. Then 10 $\mu$L of GA-MNP/PDDA/MWCNT dispersion was cast on the GCE surface and dried at room temperature. Immobilization of HRP and ChOx was carried out by dropping a 5-$\mu$L aliquot of a 940 units/mL HRP and 200 units/mL ChOx solution prepared in 0.1 M phosphate buffer, pH 7.4, onto the modified electrode surface, and the solvent was allowed to evaporate at room temperature.

**Determination of Cholesterol in Spiked Human Serum.** The solid serum was reconstituted in 1 mL of cholesterol solution (2.0, 5.0, or 7.0 mM) by mixing up to total dissolution. Serum was directly analyzed by dilution of 100-$\mu$L aliquots up to 5.0 mL with 0.1 M PBS, pH 7.5. The ChOx/HRP/GA-MNP/PDDA/MWCNT/GCE biosensor was immersed into the stirred solution and the steady-state current was measured at a constant potential of −0.05 V versus Ag/AgCl. Quantification of cholesterol was accomplished by applying the standard additions method involving the addition of 0.1 mM cholesterol aliquots.

## RESULTS AND DISCUSSION

Figure 1 (not to scale) displays graphically the different steps involved in preparation of the biosensor. Before the immobilization


dx.doi.org/10.1021/ac201466m |*Anal. Chem.* 2011, 83, 7807–7814

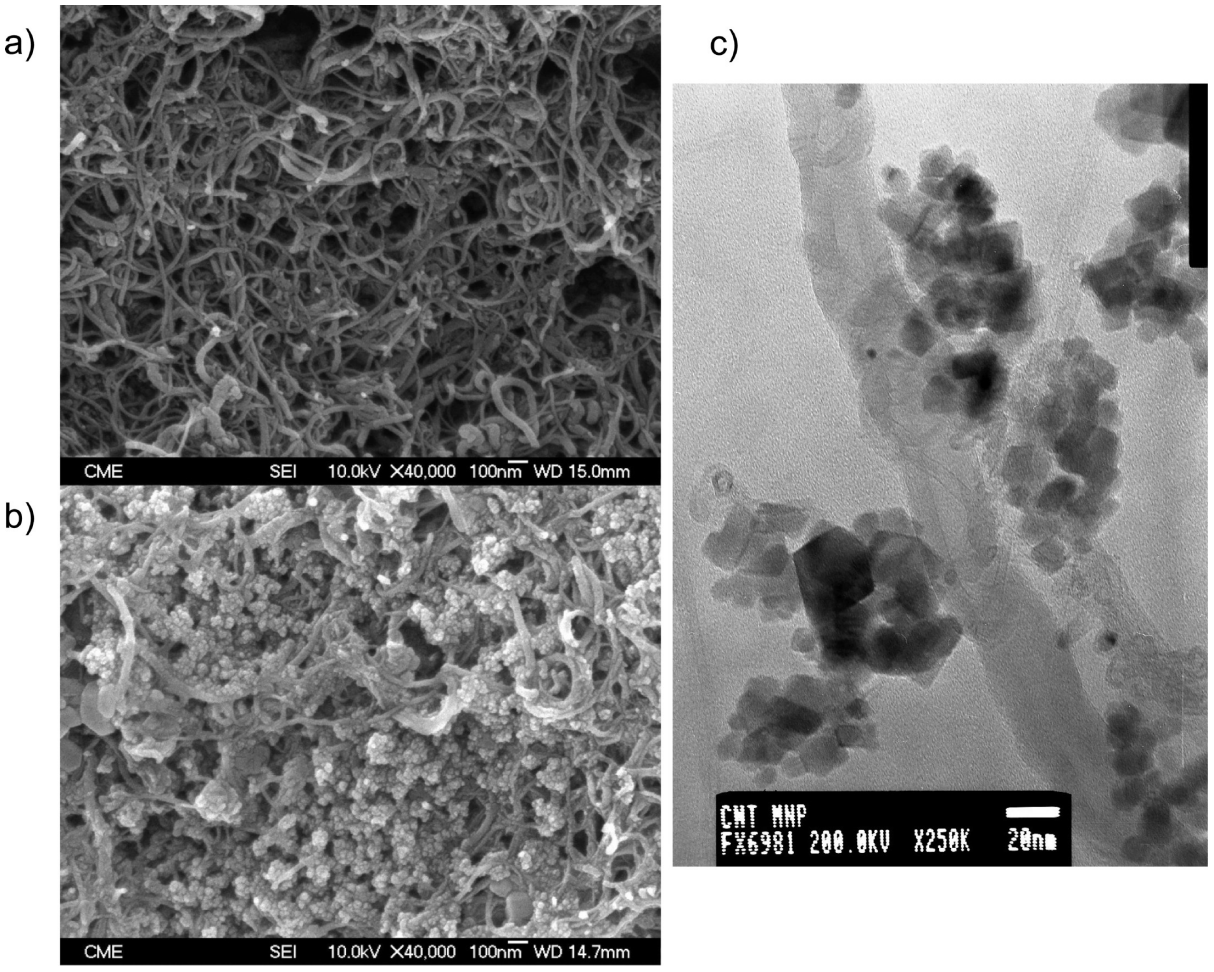


**Figure 2.** SEM images of (a) PDDA/MWCNTs and (b) GA-MNP/PDDA/MWCNTs. (c) TEM image of GA-MNP/PDDA/MWCNTs.

of enzymes, GA-MNP/PDDA/MWCNT composites were prepared. As described above, first MWCNTs were carboxylated by acid treatment. Then, PDDA/MWCNT conjugates were prepared by dispersing the carboxylated MWCNTs in an aqueous PDDA solution. Wrapping of MWCNT surface with positively charged PDDA occurred by electrostatic interaction.[25] Figure 2a shows a scanning electron microscopy (SEM) image of PDDA/MWCNTs.

Glutaraldehyde-functionalized $Fe_3O_4$/APTES magnetic nanoparticles (GA-MNPs) were prepared as described in the Experimental Section. As depicted in Figure 1, once $Fe_3O_4$ nanoparticles were synthesized, the aminosilane coupling agent APTES was incorporated as an active film to allow further functionalization by covalent binding. Fourier transform infrared (FT-IR) spectra of $Fe_3O_4$/APTES nanoparticles (Figure S1, Supporting Information) showed two absorption bands at 590 and 639 $cm^{-1}$ that are assigned to the split of the stretching vibration band of the Fe−O bonds in bulk magnetite at 570 $cm^{-1}$.[28] Also, a band at 448 $cm^{-1}$, corresponding to the hypsochromic shift of the $\upsilon_2$ band of the Fe−O bond of bulk magnetite, was observed. Moreover, Si−OH and Si−O−Si bands of the silane film appeared overlapped at 1020 $cm^{-1}$. The presence of the Si−OH groups also gave broad bands at 3698 and 3200 $cm^{-1}$, which can be attributed to the free and hydrogen-bonded hydroxyl groups linked to Si atoms. Finally, the presence of amino groups in the $Fe_3O_4$/APTES nanoparticles was evident by the band appearing at 1628 $cm^{-1}$, characteristic of $NH_2$ stretching. The magnetic properties of $Fe_3O_4$ and $Fe_3O_4$/APTES nanoparticles were also studied at room temperature by use of a vibration sample magnetometer (VSM). For both materials, the results obtained showed magnetization curves (Figure S2, Supporting Information) characteristic of superparamagnetic behavior. This implies that magnetic particles redisperse in solution without the occurrence of severe aggregation that ferromagnetic nanoparticles suffer.[28] The saturation magnetization of $Fe_3O_4$ was 60 emu/g, being slightly lower (57.3 emu/g) for $Fe_3O_4$/APTES as a consequence of the APTES coating layer. Magnetic nanoparticles were subsequently functionalized with glutaraldehyde (GA) in order to improve immobilization of the enzymes on the composite materials.

In a further step, GA-MNP/PDDA/MWCNT conjugates were prepared by interaction of the MNPs with PDDA-wrapped MWCNTs. Although the exact nature of this interaction is not completely clear, we think that the ability of PDDA to permit adhesion as well its demonstrated film-forming capability allow MNPs to be included into the film coating MWCNTs. The inherent porosity of the silane matrix coating MNPs should favor this film inclusion process. Figure 2 shows (b) SEM and (c) TEM images of these conjugates, where it can be clearly observed that MNPs are attached to the wrapped-MWCNT surface. The conjugates were cast on the GCE surface and dried at room temperature. The modified electrode was characterized by cyclic voltammetry in 0.1 M KCl solution containing 5 mM

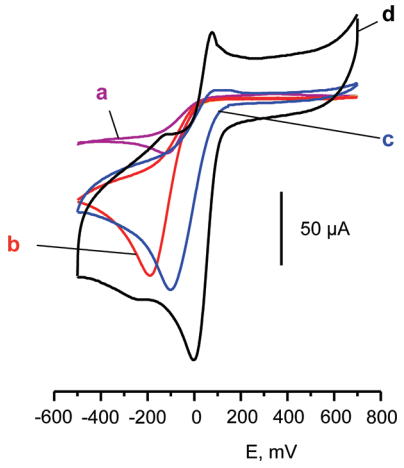


**Figure 3.** Cyclic voltammograms from solutions containing 1 mM hydroquinone and 2 mM $H_2O_2$, recorded at (a) HRP/GA/GCE, (b) HRP/GA-MNP/GCE, (c) HRP/GA/PDDA/MWCNT/GCE, and (d) HRP/GA-MNP/PDDA/MWCNT/GCE; $\upsilon$ = 50 mV/s .

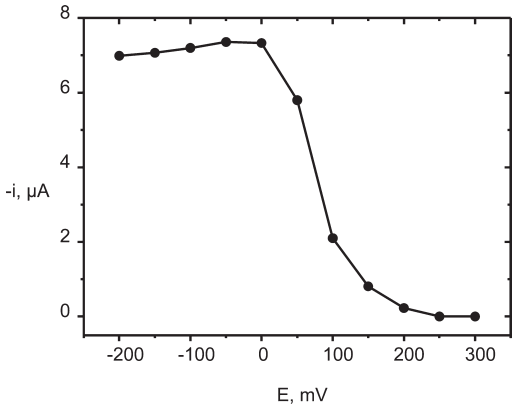


**Figure 4.** Effect of applied potential value on the amperometric detection of 0.1 mM $H_2O_2$ in the presence of 1 mM hydroquinone obtained at HRP/GA-MNP/PDDA/MWCNT/GCE.

$Fe(CN)_6^{4-/3-}$ as redox probe at different potential scan rates. The well-defined oxidation and reduction peaks (Figure S3, Supporting Information) showed peak potential values that were almost unchanged with increasing scan rate. The peak currents increased with increasing square root of the scan rate in the whole range of scan rates tested, indicating a diffusion-controlled electrode reaction process. From the $i_p$ versus $\upsilon^{1/2}$ plot, the electrochemical surface of the modified electrode was calculated by use of the Randles equation, $i_p = (2.69 \times 10^5)\, n^{3/2} A D^{1/2} C \upsilon^{1/2}$, with $D = 7.6 \times 10^{-6}$ $cm^2/s$.[29] The obtained value was 0.208 ± 0.004 ($n$ = 5) $cm^2$, which was 1.4 times higher than the electrochemical surface area calculated for the bare GCE (0.145 ± 0.007 $cm^2$). Cyclic voltammograms from 1 mM HQ solutions at different potential scan rates were also recorded (results not shown); similarly, they exhibited a linear dependence between the anodic or cathodic $i_p$ values with $\upsilon^{1/2}$. In order to evaluate the possible steric hindrance or electrostatic interference caused by the negatively charged $Fe(CN)_6^{4-/3-}$ ions on measurement of the modified electrode electrochemical surface area, this surface area was also calculated by using hydroquinone as electrochemical probe, yielding a similar value (0.205 ± 0.008 $cm^2$, $n$ = 5) to that obtained with $Fe(CN)_6^{4-/3-}$.

**HRP/ChOx/GA-MNP/PDDA/MWCNT/GCE Biosensor.** The developed electrode platform was used to construct a bienzyme biosensor for the determination of cholesterol, which implied the coimmobilization of both HRP and ChOx onto the electrode surface. As depicted in Figure 1, ChOx catalyzes the oxidation of cholesterol to form hydrogen peroxide, whose reduction is catalyzed by HRP in the presence of hydroquinone as the redox mediator, and the electrochemical reduction of the formed quinone was used for monitoring the overall reaction.

Development of the bienzyme biosensor was accomplished by performing first the evaluation of a single-enzyme HRP bioelectrode. This was carried out by following a fabrication procedure similar to that described earlier except for the ChOx incorporation. Optimization of the implied variables involved the detection of hydrogen peroxide.

Figure 3 shows cyclic voltammograms from solutions containing 1 mM hydroquinone and 2 mM $H_2O_2$, recorded with HRP biosensors constructed without MNPs and coated MWCNTs (HRP/GA/GCE), without MWCNTs (HRP/GA-MNP/GCE), without MNPs (HRP/GA/PDDA/MWCNT/GCE), and at HRP/GA-MNP/PDDA/MWCNT/GCE. As expected, a much higher reduction peak current was obtained at HRP/GA-MNP/GCE when compared with that observed for HRP/GA/GCE, which can be attributed, on the one hand, to the higher enzyme loading immobilized on the functionalized MNPs and, on the other hand, to the formation of a passivating layer when GA is directly adsorbed onto the GCE surface. The cyclic voltammogram recorded at the biosensor prepared with PDDA/MWCNTs showed a potential shift toward less negative values and a slight increase in the reduction peak current. Since impurities of metal catalysts were not detected by SEM and high-resolution TEM analysis of MWCNT, we assumed that this electrocatalytic effect was caused by the oxidized carbon surface of the nanotubes.[30,31] These effects were much more evident with HRP/GA-MNP/PDDA/MWCNT/GCE, showing the advantageous combination of electrocatalysis accrued by modification with CNTs (with subsequent enhancement of the electron-transfer rate) with efficient and stable enzyme immobilization onto the GA-functionalized MNPs. Therefore, the developed strategy was able to provide enhanced electroanalytical responses, avoiding coating of the electrode surface with cross-linking reagents.

Figure 4 shows the influence of applied potential for the amperometric detection of hydrogen peroxide in the presence of hydroquinone at HRP/GA-MNP/PDDA/MWCNT/GCE. The steady-state current exhibited the expected S-shaped behavior with almost constant high values for potentials more negative than 0.0 V. In order to minimize potential interference from other electroactive substances potentially present in serum such as ascorbic acid or uric acid, a detection potential of −0.05 V was selected for further work.

The influence of PDDA/MWCNT loading onto the GC electrode on the amperometric response of the biosensor was evaluated by preparing bioelectrodes in the 0−12 $\mu$g PDDA/MWCNT range. The obtained results (Figure S4, Supporting Information) revealed that the steady-state current practically did not vary from an 8 $\mu$g loading. This amount assured complete electrode modification and, therefore, it was selected for further work. The loading of GA-MNPs was also optimized. Figure 5a shows that the steady-state current increased up to a loading of 20 $\mu$g, while higher loadings produced a remarkable decrease,


dx.doi.org/10.1021/ac201466m |*Anal. Chem.* 2011, 83, 7807–7814

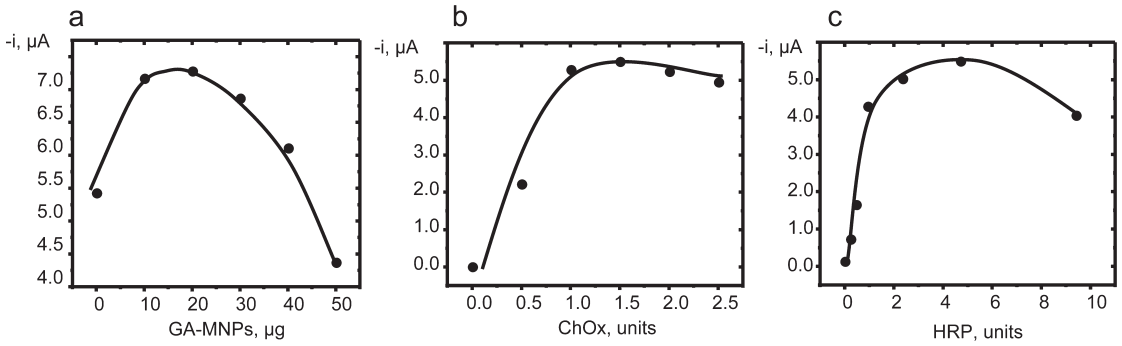


**Figure 5.** Optimization of (a) GA-MNP, (b) ChOx, and (c) HRP loadings. Conditions: (a) 8 $\mu$g of PDDA/MWCNTs, 0.1 mM $H_2O_2$, 1 mM hydroquinone, 9.4 units of HRP; (b) 0.2 mM cholesterol and 4.7 units of HRP; (c) 0.2 mM cholesterol and 1 unit of ChOx. Each plotted point is the mean value of the measurements carried out with three different bioelectrodes.

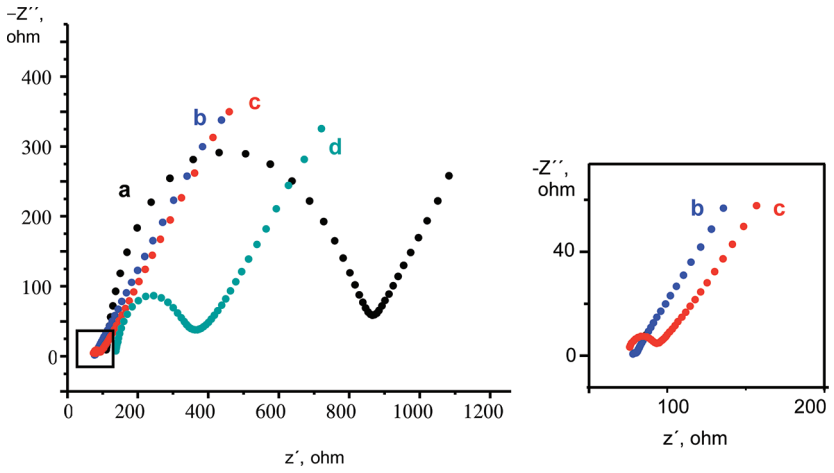


**Figure 6.** Nyquist plots recorded from a 5 mM $[Fe(CN)_6]^{3-/4-}$ 0.1 M KCl solution at (a) bare GCE, (b) PDDA/MWCNT/GCE, (c) GA-MNP/PDDA/MWCNT/GCE, and (d) HRP/ChOx/GA-MNP/PDDA/MWCNT/GCE.

probably due to blocking of the electrode active surface. Thus, 20 $\mu$g was selected for further work.

The optimized parameters mentioned above were taken for the subsequent construction of the bienzyme ChOx/HRP biosensor. Therefore, both the ChOx and HRP loadings were also optimized by measuring the amperometric responses to 0.2 mM cholesterol of different bienzyme biosensors prepared with a constant 4.7 units of HRP loading and various ChOx loadings ranging between 0 and 2.5 units. Figure 5b shows that the steady-state current increased with the amount of ChOx up to approximately 1 unit, and then it slightly decreased as a probable consequence of the electrode blocking. A similar set of experiments was performed by constructing biosensors with 1 unit of ChOx and various HRP loadings between 0 and 9.4 units. As can be observed in Figure 5c, the largest response was achieved for 4.7 units of HRP. Accordingly, 1 unit of ChOx and 4.7 units of HRP were selected as enzyme loadings for the bienzyme biosensor preparation.

The step-by-step biosensor construction was also characterized by electrochemical impedance spectroscopy. Figure 6 compares the Nyquist plots obtained in a 5 mM $[Fe(CN)_6]^{3-/4-}$ 0.1 M KCl solution for bare GCE, PDDA/MWCNT/GCE, GA-MNP/PDDA/MWCNT/GCE, and ChOx/HRP/GA-MNP/PDDA/MWCNT/GCE. As can be observed, the quasi-ideal capacitor behavior observed for PDDA/MWCNT/GCE, with a very small electron-transfer resistance ($R_{ct}$) value ($2 \pm 2\ \Omega$), changed upon incorporation of GA-MNPs with a slight increase in the $R_{ct}$ value ($21 \pm 6\ \Omega$), which evidenced that the layer of GA-functionalized nonconducting MNPs blocked partially the electrode surface but with sufficient available conducting sites to allow the electrochemical reaction to be performed. Furthermore, as expected, incorporation of the enzymes on the functionalized MNPs produced a noticeable increase in the electron-transfer resistance ($R_{ct} = 216 \pm 32\ \Omega$), which confirmed the successful immobilization of the enzymes.

The study of the influence of pH on the amperometric response of the biosensor (results not shown) demonstrated that the highest current was attained at pH 7.5. Furthermore, the hydroquinone concentration in solution was also optimized. The steady-state current dramatically increased from 0 to 0.1 mM, showing a much lower increase up to 2 mM hydroquinone concentration. Therefore, 0.50 mM was selected as the concentration of redox mediator to be used in subsequent work.

**Analytical Characteristics of HRP/ChOx/GA-MNP/PDDA/MWCNT/GCE Biosensor.** By use of the optimized working parameters, a linear calibration plot for cholesterol ($r = 0.996$) was obtained in the 0.01−0.95 mM concentration range (Figure 7). The limit of detection (LOD), 0.85 $\mu$M, was calculated according

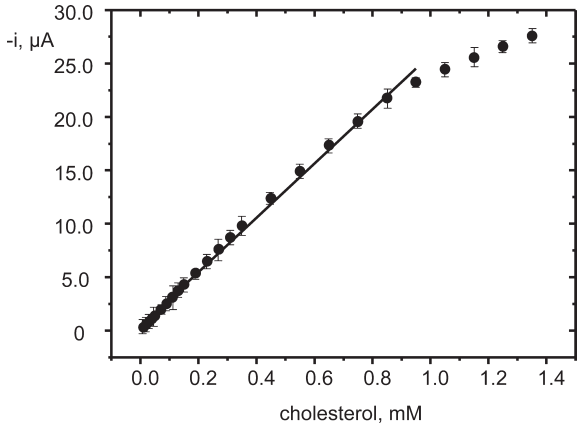


**Figure 7.** Calibration plot for cholesterol obtained at the HRP/ChOx/GA-MNP/PDDA/MWCNT/GCE biosensor.

to the $3s_b/m$ criterion, where $s_b$ was estimated as the standard deviation ($n = 10$) of the amperometric signals corresponding to different solutions of cholesterol at the lowest concentration level in the range of linearity (i.e., 0.01 mM) and $m$ was the slope of the calibration graph, 25.4 $\mu$A/mM. The sensitivity achieved can be ranged among the best ones when compared with data reported in the literature for other CNT-based cholesterol biosensors. The slope value is much higher than that achieved with a layer-by-layer PPD(PDDA/ChOx)$_n$/MWCNT/AuE configuration ($m$ = 0.175 $\mu$A/mM)[10] at a detection potential of +0.7 V, as well as those obtained with a ChOx/PANI/MWCNT/ITO electrode ($m$ = 6.8 $\mu$A/mM at $E_{det}$ = 0.28 V),[16] and with a biosensor involving vertically aligned CNTs with immobilized ChOx, HRP, and cholesterol esterase ($m$ = 8.5 $\mu$A/mM at $E_{det}$ = 0.4 V).[32] Only the slope value reported for a layer-by-layer PDDA(MWCNT/ChOx)$_5$/graphite biosensor configuration was higher ($m$ = 136.5 $\mu$A/mM).[23] Nevertheless, it should be noted that the detection limit achieved with the HRP/ChOx/GA-MNP/PDDA/MWCNT/GCE biosensor was 35 times lower and the range of linearity was considerably wider.

Figure 7 shows typical Michaelis−Menten kinetics behavior, as was confirmed by calculating the $x$ parameter, 0.98, from the corresponding Hill plots ($[\log (i_{max}/i) - 1)]$ versus the log of the substrate concentration). Consequently, the apparent Michaelis−Menten constant, ($K_M^{app}$) and the maximum reaction rate value ($V_m$) were calculated from the corresponding Lineweaver−Burk plot. The obtained values were $K_M^{app}$ = 1.57 mM and $V_m$ = 47.6 $\mu$A. This $K_M^{app}$ value was 2 times higher than that reported recently for ChOx in aqueous solutions.[33] However, it is important to remark that the obtained $K_M^{app}$ value was significantly lower than those reported for other electrode configurations such as the designs involving a PPD(PDDA/ChOx)$_n$/MWCNT/AuE biosensor (7.17 mM)[24] and ChOx immobilized on poly(vinylferrocenium) perchlorate film-coated Pt electrodes (3.9 mM).[34] This fact suggests that the Michaelis−Menten equilibrium was favored in our electrode design, probably as a consequence of the microenvironment provided by GA-MNPs.

Regarding the stability of the ChOx/HRP/GA-MNP/PDDA/MWCNT/GCE biosensor, different aspects were evaluated. First, the repeatability of successive amperometric measurements for five different 0.1 mM cholesterol solutions carried out with the same biosensor was checked. A relative standard deviation value (RSD) of 5.8% was calculated for the steady-state current.

**Table 1. Results Obtained in Analysis of Human Sera with the HRP/ChOx/GA-MNP/PDDA/MWCNT/GCE Biosensor**

| | cholesterol, mM | | | | |
|---|---|---|---|---|---|
| sample[a] | added | found | avg found | RSD, % | recovery, % |
| 1 | 2.0 | 2.01, 2.16, 1.87, 1.97, 2.09 | 2.02 | 5.5 | 101.0 |
| 2 | 5.0 | 5.02, 4.84, 5.13, 5.28, 4.75 | 5.01 | 4.3 | 100.2 |
| 3 | 7.0 | 7.18, 7.17, 7.61, 6.94, 7.27 | 7.23 | 3.3 | 103.3 |

[a] Samples were spiked with cholesterol at the 2.0 (sample 1), 5.0 (sample 2), and 7.0 (sample 3) mM concentration levels.

Furthermore, the reproducibility of the responses obtained with five different biosensors was also evaluated. The mean value of the performed measurements yielded a RSD value of 8.2%. Moreover, the lifetime of a single ChOx/HRP/GA-MNP/PDDA/MWCNT/GCE biosensor was checked by performing three daily measurements for 0.05 mM cholesterol. The amperometric response did not show significant differences (within ±3× standard deviation of the mean value measured the first day) for at least 14 days, without any regeneration procedure applied to the bioelectrode surface. Similar results were obtained when the assay was performed with 0.1 mM cholesterol. This working stability is remarkably better than that reported for other CNT-based biosensors (1 week),[19,20,23] and it can be attributed to the successful enzyme immobilization strategy on the GA-MNPs retaining their biological activity

The effect of temperature on the bienzyme biosensor response was studied by measuring the steady-state current of 0.1 mM cholesterol solutions at temperatures ranging from 25 to 60 °C. The current exhibited a fast increase with temperature up to 45 °C and decreases for higher temperatures, probably due to denaturation of the enzymes. From the ln $i$ versus $1/T$ plot in the 25−40 °C range, and according to the Arrhenius equation, an activation energy value of 10.68 kJ/mol was calculated. This value is lower than that obtained when ChOx was immobilized onto MWCNT/$SiO_2$/Chit composites, $E_a$ = 42.6 kJ/mol,[20] and much lower than that given for the immobilization of ChOx onto polyaniline, $E_a$ = 71.1 kJ/mol,[35] thus revealing the high enzyme activity when GA-MNP/PDDA/MWCNT was used as immobilization substrate.

**Determination of Cholesterol in Spiked Human Serum.** As a straightforward real application of the bienzyme bioelectrode, the analysis of human serum spiked with cholesterol at three different concentration levels covering usual ranges in human sera, 2.0, 5.0, and 7.0 mM, was accomplished. As described in the Experimental Section, a 100-$\mu$L aliquot of serum was diluted with 0.1 M PBS (pH 7.5) solution up to 5.0 mL, and the determination of cholesterol was performed by applying the standard additions method involving the addition of 0.1 mM cholesterol aliquots. Table 1 summarizes the obtained results, where it can be seen that mean recoveries ranged between 100% and 103% with relative standard deviations of 5.5%, 4.3%, and 3.3%. These results demonstrated fairly well the usefulness of the developed ChOx/HRP/GA-MNP/PDDA/MWCNT/GCE biosensor for determination of free cholesterol in serum samples with practically no sample treatment.

## CONCLUSIONS

The novel electrochemical interfaces constructed from functionalized MNPs and properly wrapped CNTs have been

demonstrated to be useful for the preparation of multienzyme biosensors. The excellent analytical performance for determination of cholesterol achieved with the bienzyme biosensor constructed by immobilizing ChOx and HRP on the developed transducer platforms allows us to conclude that the strategy can be successfully employed for such a purpose. The coupling of beneficial properties of the modified MNPs, to improve the immobilization of the enzymes onto the composite material, with the electrocatalytic effect and stability provided by PDDA-wrapped carbon nanotubes leads to an enhanced sensitivity of the biosensing platform compared to that achieved with other methods described in the literature using biosensors prepared with carbon nanotubes solely. It is hoped that the successful strategy developed for the first time in this work may be easily extended for the preparation of other multyenzyme biosensing designs.

## ■ ASSOCIATED CONTENT

**Supporting Information.** Four figures, showing FT-IR spectrum, magnetization curves, cyclic voltammograms, and effect of PDDA/MWCNT loading on amperometric detection as described in the text. This material is available free of charge via the Internet at http://pubs.acs.org.

## ■ AUTHOR INFORMATION

**Corresponding Author**
*Fax: +34913944329. E-mail: pingarro@quim.ucm.es.

## ■ ACKNOWLEDGMENT

R.V. acknowledges a Ramón & Cajal contract from the Spanish Ministry of Science and Innovation. Financial support from the Spanish Ministerio de Ciencia e Innovación (Projects DPS2008-07005-C02-01, CTQ2009-12650, and CTQ2009-09351) and Comunidad de Madrid S2009/PPQ-1642, program AVANSENS, is gratefully acknowledged.

## ■ REFERENCES

(1) Agüí, L.; Yáñez-Sedeño, P.; Pingarrón, J. M. *Anal. Chim. Acta* **2008**, *622*, 15–20.
(2) Li, D.; Teoh, W. Y.; Gooding, J. J.; Selomulya, C.; Amal, R. *Adv. Funct. Mater.* **2010**, *20*, 1767–1777.
(3) Cheng, Y.; Liu, Y.; Huang, J.; Li, K.; Xian, Y.; Zhang, W.; Jin, L. *Electrochim. Acta* **2009**, *54*, 2588–2594.
(4) Qu, S.; Wang, J.; Kong, J.; Yang, P.; Chen, G. *Talanta* **2007**, *71*, 1096–1102.
(5) Theres Baby, T.; Ramaprabhu, S. *Talanta* **2010**, *80*, 2016–2022.
(6) Li, J.; Wei, X.; Yuan, Y. *Sens. Actuators, B* **2009**, *139*, 400–406.
(7) Lu, B.-W.; Chen, W.-C. *J. Magn. Magn. Mater.* **2006**, *304*, e400–e402.
(8) Yang, L.; Ren, X.; Tang, F.; Zhang, L. *Biosens. Bioelectron.* **2009**, *25*, 889–895.
(9) Piao, Y.; Jin, Z.; Lee, D.; Lee, H.-J.; Na, H.-B.; Hyeon, T.; Oh, M.-K.; Kim, J.; Kim, H.-S. *Biosens. Bioelectron.* **2011**, *26*, 3192–3199.
(10) Ran, X.-Q.; Yuan, R.; Chai, Y.-Q.; Hong, C.-L.; Qian, X.-Q. *Colloids Surf., B* **2010**, *79*, 421–426.
(11) Zhou, Y. L.; Li, Y. Z. *Colloids Surf., A.* **2004**, *233*, 129–135.
(12) Li, N.; Zhao, H. W.; Yuan, R.; Peng, K. F.; Chai, Y. Q. *Electrochim. Acta* **2008**, *54*, 235–241.
(13) Muthirulam, P.; Velmurugan, R. *Colloids Surf., B* **2011**, *83*, 347–354.
(14) Qin, X.; Wang, H.; Wang, X.; Li, S.; Miao, Z.; Huang, N.; Chen, Q. *Mater. Sci. Eng., C* **2009**, *29*, 1453–1457.
(15) Arya, S. K.; Datta, M.; Malhotra, B. D. *Biosens. Bioelectron.* **2008**, *23*, 1083–1100.
(16) Dhand, C.; Arya, S. K.; Datta, M.; Malhotra, B. D. *Anal. Biochem.* **2008**, *383*, 194–199.
(17) Gopalan, A. I.; Lee, K. P.; Ragupathy, D. *Biosens. Bioelectron.* **2009**, *24*, 2211–2217.
(18) Yang, M.; Yang, Y.; Yang, H.; Shen, G.; Yu, R. *Biomaterials* **2006**, *27*, 246–255.
(19) Yang, M.; Yang, Y; Qu, F.; Lu, Y.; Shen, G.; Yu, R. *Anal. Chim. Acta* **2006**, *571*, 211–217.
(20) Tan, X.; Li, M.; Cai, P.; Luo, L.; Zou, X. *Anal. Biochem.* **2005**, *337*, 111–120.
(21) Tsai, Y.-C.; Chen, S.-Y.; Lee, C.-A. *Sens. Actuators, B* **2008**, *135*, 96.
(22) Solanki, P. R.; Kaushik, A.; Ansari, A. A.; Tiwari, A.; Malhotra, B. D. *Sens. Actuators, B* **2009**, *137*, 727–735.
(23) Manjunatha, R.; Nagaraju, D. H.; Suresh, G. S.; Melo, J. S.; D'Souza, S. F.; Venkatesha, T. V. *J. Electroanal. Chem.* **2011**, *651*, 24–29.
(24) Guo, M.; Chen, J.; Li, J.; Nie, L.; Yao, S. *Electroanalysis* **2004**, *16*, 1992–1998.
(25) Cui, R.; Huang, H.; Yin, Z; Gao, D.; Zhu, J.-J. *Biosens. Bioelectron.* **2008**, *23*, 1666–1673.
(26) Kang, Y. S.; Risbud, S.; Rabolt, J. F.; Stroeve, P. *Chem. Mater.* **1996**, *8*, 2209–2211.
(27) Villalonga, R.; Villalonga, M. L.; Díez, P.; Pingarrón, J. M. *J. Mater. Chem.* **2011**, *21*, 12858–12864.
(28) Cao, H.; He, J.; Deng, L.; Gao, X. *Appl. Surf. Sci.* **2009**, *255*, 7974–7980.
(29) Gooding, J. J.; Praig, V. G.; Hall, E. A. H. *Anal. Chem.* **1998**, *70*, 2396–2402.
(30) Haddad, R.; Cosnier, S.; Maaref, A.; Holzinger, M. *Sens. Lett.* **2009**, *7*, 801–805.
(31) Li, J.; Yu, Q.; Peng, T. *Anal. Sci.* **2005**, *21*, 377–381.
(32) Wisitsoraat, A.; Karuwan, C.; Wong-ek, K.; Phokharatkul, D.; Sritongkham, P.; Tuantranont, A. *Sensors* **2009**, *9*, 8658–8668.
(33) Sun, Y.; Yang, H.; Wang, W. *Biotechnol. Lett.* **2011**, *33*, 2049–2055.
(34) Özer, B. C.; Özyörük, H.; Çelebi, S. S.; Yıldız, A. *Enzym. Microb. Technol.* **2007**, *40*, 262–265.
(35) Wang, H. Y.; Mu, S. L. *Sens. Actuators, B* **1999**, *56*, 22–30.